Available online at www.sciencedirect.com
SCIENCE DIRECT®
Chemical Physics Letters 369 (2003) 8–15
CHEMICAL PHYSICS LETTERS
www.elsevier.com/locate/cplett

Experimental implementation of Grover's search algorithm using efficient quantum state tomography

Ranabir Das [a], T.S. Mahesh [a], Anil Kumar [a,b,*]

[a] *Department of Physics, Indian Institute of Science, Bangalore 560012, India*
[b] *Sophisticated Instruments Facility, Indian Institute of Science, Bangalore 560012, India*

Received 3 October 2002; in final form 2 November 2002

Abstract

Quantum state tomography is an important step in quantum information processing. For ensemble systems such as nuclear magnetic resonance (NMR), quantum state tomography implies a characterization of the complete density matrix. For an *n*-qubit system the size of density matrix and hence the amount of information required for tomography is exponential in '*n*'. Since, only single qubit single quantum elements are observable in NMR, exponential number of one dimensional experiments with readout pulses to rotate the unobservable elements into observables, have earlier been used to map the density matrix. Recently a novel method of efficient tomography has been developed, which requires constant experimental time for any number of qubits. In this method, all off diagonal elements of the density matrix are mapped using a two-dimensional Fourier Transform NMR experiment and all diagonal elements using a one dimensional experiment. In this Letter, the novel method of tomography is demonstrated experimentally while implementing Grover's search algorithm on a two-qubit system.

1. Introduction

In 1982 Feynman pointed out that it would be more efficient to simulate the behavior of a quantum system using a quantum, rather than a classical device [1]. The idea of a purpose-built quantum device which could simulate the physical behavior of a quantum system, attracted immediate attention [2]. In the early 1990s, several quantum algorithms like Deutsch-Jozsa algorithm, Shor's factorization algorithm and Grover's search algorithm were developed [3–5]. Since then researchers have strived to develop a quantum device in physical systems whose evolution is coherent, unitary and controllable. Nuclear magnetic resonance (NMR) has successfully demonstrated several quantum algorithms and simulations for small number of qubits [6–20]. However, scaling to large number of qubits poses several challenges. One of them is 'quantum state tomography' [9]. At the end of an algorithm and often during the flow of an algorithm, one needs to measure the results and estimate errors. This is achieved by measuring the

* Corresponding author. Fax: (SIF) +91-80-3601550, (PHY) +91-80-360-2602.
E-mail address: anilnmr@physics.iisc.ernet.in (A. Kumar).

0009-2614/03/$ - see front matter © 2003 Elsevier Science B.V. All rights reserved.
doi:10.1016/S0009-2614(02)01895-X

state of the system, known as state tomography. In ensemble systems such as NMR, state tomography amounts to characterization of density matrix of the system.

With the increase in size of the system the amount of information to be acquired increases exponentially; for an n-qubit system the size of the density matrix is $K = 2^n \times 2^n$. Of these K elements there are $M = (2^n - 1)(2^{n-1} + 1)$ independent elements. Of these there are $(n2^{n-1})$ one qubit single quantum observable elements. To measure the remaining elements, exponential number of one-dimensional experiments with readout pulses to rotate the unobservables into observables, have been used [16–18]. Recently a novel method of state tomography using a two-dimensional Fourier transform technique has been developed [19]. This protocol requires a one-dimensional experiment to measure all the diagonal elements of the density matrix and a two-dimensional experiment to measure all the off diagonal elements. The number of t_1 increments in the two dimensional either remain constant or increase linearly with the number of qubits to maintain the same level of digital resolution. In this work we demonstrate this protocol experimentally while implementing Grover's search algorithm on a two-qubit system, tomographing the state of the system at initial, intermediate and final steps of the algorithm. Grover's search algorithm has earlier been implemented on a two-qubit system, where the state of the system was tomographed using the earlier method of Chuang et al. [17].

2. Quantum state tomography

The new method of quantum state tomography requires two experiments (Fig. 1) [19]. The experiment for measuring the diagonal elements, Fig. 1a, starts with a gradient pulse, which destroys all off-diagonal elements. The small angle detection (10°) radio-frequency (r.f.) pulse converts differences in diagonal elements into detectable single quantum coherences whose amplitudes allow calculation of the diagonal elements. The experiment for measuring off-diagonal elements (Fig. 1b) starts with the given density matrix, which is allowed to evolve for a time t_1. At the end of t_1, a 90° r.f. pulse transforms every element of the density matrix into all other elements including diagonal elements. The gradient pulse destroys all the off diagonal elements, retaining only the diagonal elements. These diagonal elements are transformed by a 45° pulse into observable single-quantum coherences, which are read as a function of time-variable t_2. A series of experiments are performed, each starting with the initial density matrix to be tomographed by systematic incrementation of the t_1 period and collecting two-dimensional time domain data set s(t_1, t_2). This data set is double Fourier analysed with respect to both these time

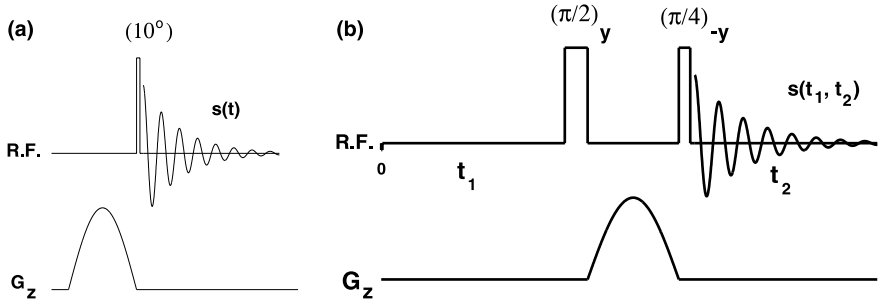

Fig. 1. Pulse sequence for measurement of (a) diagonal elements and (b) off-diagonal elements of the density matrix. The experiment (a) is a single measurement as a function of time-variable t. Upon Fourier transform of $s(t)$ one obtains a spectrum (one-dimensional) which yields all the diagonal elements of the density matrix. In experiment (b) a series of experiments are performed with incremented t_1 period. A complete set of data $s(t_1, t_2)$ is collected with time-variables t_1 and t_2, which on Fourier transform with respect to both these time variables, yields a data $S(\omega_1, \omega_2)$ which is a function of two frequency variables ω_1 and ω_2. This spectrum has a complete information of all off-diagonal elements.

variables, yielding a two-dimensional frequency domain spectrum $S(\omega_1, \omega_2)$ [21]. The two-dimensional spectrum $S(\omega_1, \omega_2)$ contains along ω_2 all allowed single quantum transitions and along ω_1, the contribution of every off-diagonal elements of the density matrix to these transitions, dispersed and displayed in the ω_1 frequency axis according to their specific evolution frequency in the time-domain t_1 [19].

3. Grovers search algorithm

The aim of a search problem is to retrieve a data element satisfying a given condition from an unsorted database. The most efficient classical algorithm would search each item one by one and would take on an average of $0.5N$ steps before finding the requisite item out of the N items. It is shown by Grover [5] that by having the elements of the database in a coherent superposition of states, one can search an object in $O(\sqrt{N})$ quantum mechanical steps.

Grover's search algorithm has three steps. First step creates an uniform superposition of all states (items) such that each state has equal amplitude. Second step has two operators; *conditional sign-flip* 'C_{ij}' and *inversion* 'D' about mean. The *conditional sign-flip* operator flips the sign of desired state. The *inversion* operator inverts every state about the mean amplitude of all the states. The second step has to be iterated $O(\sqrt{N})$ times. The third step is to measure the resulting state. The measured state will be the desired state with high probability (the details of the algorithm are in [5]).

Grover's search algorithm is implemented here on a two-qubit system, wherein the algorithm requires only one iteration of the second step. The experiment has been implemented previously by Chuang et al. [17], where tomography of the states

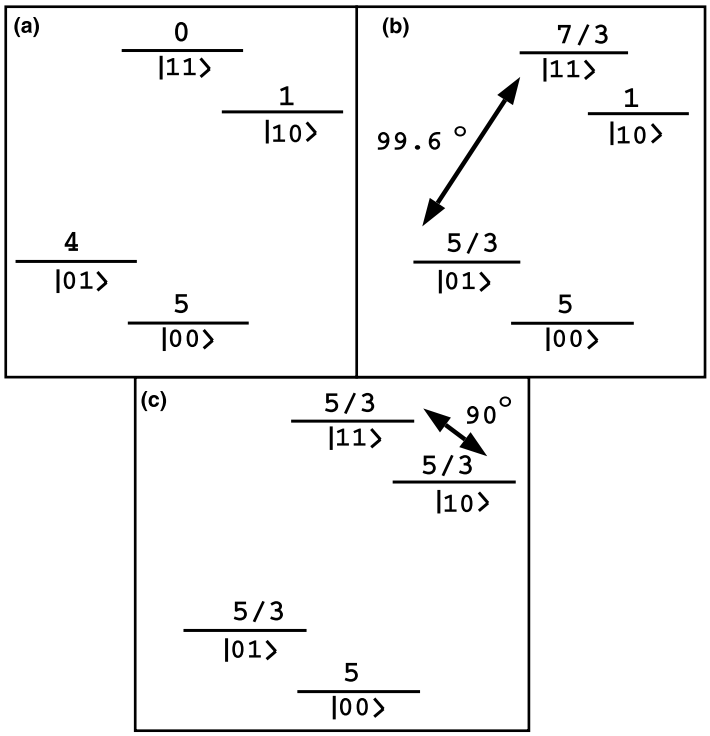

Fig. 2. Preparation of $|00\rangle$ pseudopure state by spatial averaging technique using transition selective pulses. Populations of different states in (a) thermal equilibrium, (b) after a 99.6° pulse on transition $|01\rangle \leftrightarrow |11\rangle$, followed by (c) 90° pulse on transition $|10\rangle \leftrightarrow |11\rangle$. A gradient is applied finally to kill all unwanted coherences created during the process. The final population distribution of (c) corresponds to a $|00\rangle$ pseudopure state.

of the system was performed using nine sets of one-dimensional experiments. In this work, we have tomographed the state of the system at initial, intermediate and final steps of the algorithm using two-dimensional Fourier transform technique described in the above section. The sample used is *N*,*N*-dimethyl formamide (^{13}C labeled) dissolved in $CDCl_3$. The spin 1/2 nuclei ^{13}C and ^{1}H (attached to ^{13}C) act as the two qubits. The *J*-coupling between them is $J = 192$ Hz. The resonance lines from other nuclei and solvent do not interfere with the spectrum of the two qubits. The schematic energy level diagram of the system is given in Fig. 2. The $|00\rangle$ pseudopure state was created by spatial

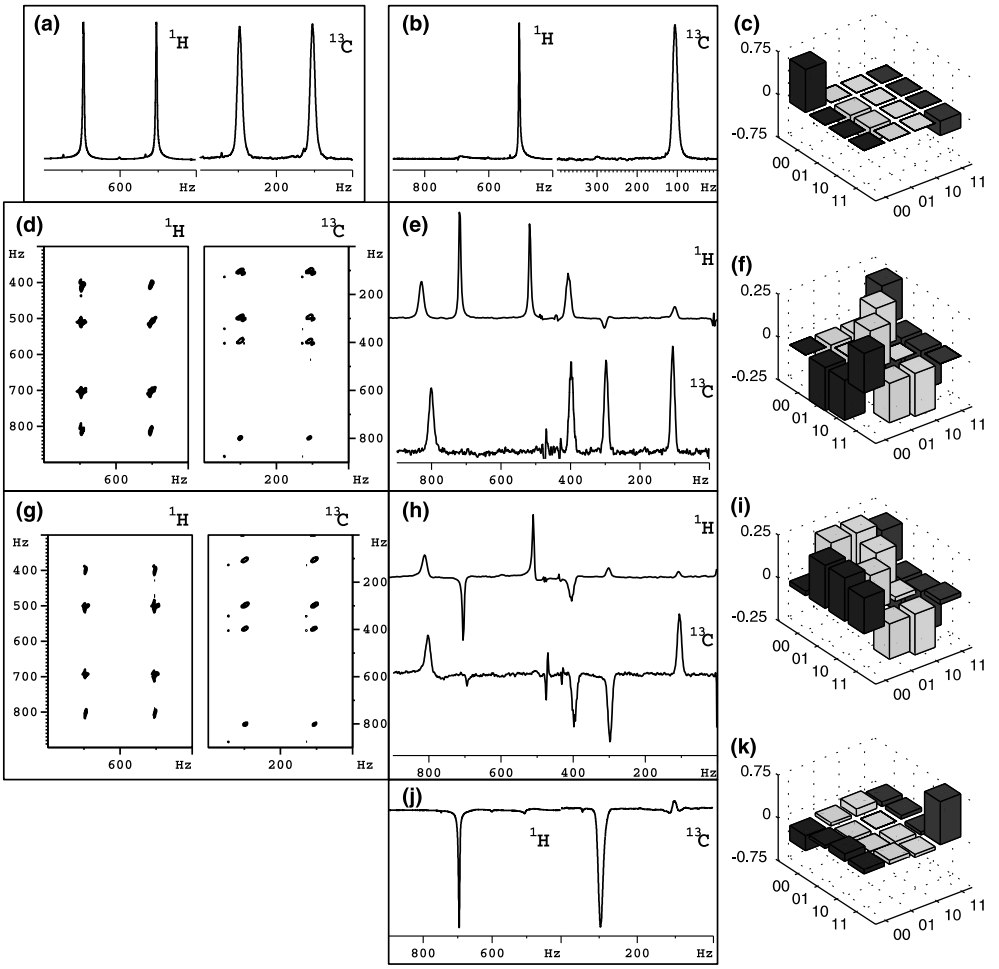

Fig. 3. Experimental implementation of Grover's search algorithm on a two-qubit system (^{1}H–^{13}C) of *N*,*N*-dimethyl formamide (^{13}C labeled). The offset resonance frequency are $\Omega_{1H} = 600$ Hz and $\Omega_{13C} = 200$ Hz, while the coupling is $J = 192$ Hz. (a) ^{1}H, ^{13}C equilibrium spectra obtained using 10° detection pulse. (b) ^{1}H and ^{13}C spectra corresponding to $|00\rangle$ pseudopure state prepared using spatial averaging method described in the text and Fig. 2. (c) The tomograph of the pseudopure state of (b). (d) ^{1}H, ^{13}C two-dimensional spectra obtained (after creation of uniform superposition from $|00\rangle$ pseudopure state) using method of Fig. 1b. (e) Cross-sections parallel to ω_1 of (d) taken at $\omega_2 = 504$ Hz ($\Omega_{1H} - J/2$) for ^{1}H and $\omega_2 = 104$ Hz ($\Omega_{13C} - J/2$) for ^{13}C. (f) The tomograph of the state of uniform superposition (calculated from (d)). (g) ^{1}H – ^{13}C, two-dimensional spectra, after conditional sign flip, obtained using scheme of Fig. 1b. (h) cross-sections of (g) similar to (e). (i) Tomograph of the state after conditional flip calculated from (g). (j) The spectra corresponding to final state of Grover's search algorithm and its tomograph (k). All the tomographs shown in Figs (c), (f), (i) and (k) are measured using the scheme of Fig. 1.

averaging technique using transition selective pulses [8,20]. A 99.6° transition selective pulse on transition $|01\rangle \leftrightarrow |11\rangle$ followed by a 90° pulse on the transition $|10\rangle \leftrightarrow |11\rangle$ equalizes the populations of the $|01\rangle$, $|10\rangle$, and $|11\rangle$ states (Fig. 2). The population of $|00\rangle$ state remains unaffected and different from all the other states, hence establishing $|00\rangle$ pseudopure state. It may be noted that in the earlier experiment by Chuang et al. [17], temporal averaging technique [7] was used to create the pseudopure state. In the 2-qubit case temporal averaging requires three different experiments, cyclically permuting the populations of three states and summing the result.

The created pseudopure state $|00\rangle$ can be expressed as

$$|\psi_1\rangle = |00\rangle = \begin{pmatrix} 1 \\ 0 \\ 0 \\ 0 \end{pmatrix}. \tag{1}$$

The spectra corresponding to the equilibrium and the pseudopure state of the 2 qubit $^{13}C - {}^{1}H$ system are shown in Fig. 3a,b, respectively. The tomographed density matrix of the pseudopure state using scheme of Fig. 1 is shown by a bar plot in Fig. 3c. To create uniform superposition, we apply Hadamard operator H. Hadamard operator transforms a qubit in state $|0\rangle$ to $\frac{1}{\sqrt{2}}(|0\rangle + |1\rangle)$ and in state $|1\rangle$ to $\frac{1}{\sqrt{2}}(|0\rangle - |1\rangle)$. The Hadamard operator for jth qubit is given by [10]

$$H_j = \frac{1}{\sqrt{2}} \begin{pmatrix} 1 & 1 \\ 1 & -1 \end{pmatrix}. \tag{2}$$

Application of Hadamard operator to a pseudopure state creates the state of uniform superposition. For example in a 2-qubit system one obtains

$$|\psi_2\rangle = (H_1 \otimes H_2)|\psi_1\rangle = \frac{1}{2} \begin{pmatrix} 1 & 1 & 1 & 1 \\ 1 & -1 & 1 & -1 \\ 1 & 1 & -1 & -1 \\ 1 & -1 & -1 & 1 \end{pmatrix} \begin{pmatrix} 1 \\ 0 \\ 0 \\ 0 \end{pmatrix} = \frac{1}{2} \begin{pmatrix} 1 \\ 1 \\ 1 \\ 1 \end{pmatrix}. \tag{3}$$

The Hadamard operator is realized by the pulses $(\pi/2)_{-y}(\pi)_x$ (pulses are on both the qubits and are applied from right to left), where $(\pi/2)_{-y}$ means an anticlockwise rotation by $\pi/2$ about the $-y$ axis, and has the operator form of $(\pi/2)_{-y} = \exp(\mathrm{i}\frac{\pi}{2}\sigma_y/2)$ [10]. The state $|\psi_2\rangle$ was also tomographed by experiments of Fig. 1. Fig. 3d shows the two-dimensional spectra corresponding to $|\psi_2\rangle$ obtained by experiment of Fig. 1b. Fig. 3e shows the cross-sections of Fig. 3d parallel to ω_1, at one transition of each qubit along ω_2. The protocol of tomography assumes ideal pulses. To account for the imperfection of r.f. pulses, a direct detection allows one to measure the single quantum elements of the density matrix which were then used to normalize all the other off-diagonal elements of the density matrix obtained by the two-dimensional experiment [19]. The tomographed complete density matrix is shown alongside Fig. 3f.

The conditional sign-flip step changes the sign of the searched state. The operator corresponding to the search of state $|11\rangle$ is given by;

$$C_{11} = \begin{pmatrix} 1 & 0 & 0 & 0 \\ 0 & 1 & 0 & 0 \\ 0 & 0 & 1 & 0 \\ 0 & 0 & 0 & -1 \end{pmatrix}. \tag{4}$$

This operator is realized using J-evolution by the sequence $(\frac{\pi}{2})_y(\frac{\pi}{2})_{-x}(\frac{\pi}{2})_{-y}(\frac{\tau}{2})(\pi)_{-x}(\frac{\tau}{2})$ (up to an overall irrelevant phase factor) [17]. The pulses are hard pulses applied on both the qubits. The last three terms in the sequence allow the system to evolve only under the coupling Hamiltonian, the chemical shifts being refocused by the hard $(\pi)_{-x}$ pulse. The operator corresponding to evolution under coupling Hamiltonian for a time $\tau = 1/2J$ is

$$\exp(\mathrm{i}2\pi J I_{1z} \otimes I_{2z}\tau) = \frac{1}{\sqrt{2}} \begin{pmatrix} 1+\mathrm{i} & 0 & 0 & 0 \\ 0 & 1-\mathrm{i} & 0 & 0 \\ 0 & 0 & 1-\mathrm{i} & 0 \\ 0 & 0 & 0 & 1+\mathrm{i} \end{pmatrix}. \tag{5}$$

The operator corresponding to the first three pulses is:

$$\begin{aligned}\left(\frac{\pi}{2}\right)_y\left(\frac{\pi}{2}\right)_{-x}\left(\frac{\pi}{2}\right)_{-y} &= \exp(-i\pi/2(I_{1y}+I_{2y}))\\ &\quad\times\exp(i\pi/2(I_{1x}+I_{2x}))\\ &\quad\times\exp(i\pi/2(I_{1y}+I_{2y}))\\ &= \frac{1}{8}\begin{pmatrix}1 & 1 & 1 & 1\\ -1 & 1 & -1 & 1\\ -1 & -1 & 1 & 1\\ 1 & -1 & -1 & 1\end{pmatrix}\\ &\quad\times\begin{pmatrix}1 & -i & -i & -1\\ -i & 1 & -1 & -i\\ -i & -1 & 1 & -i\\ -1 & -i & -i & 1\end{pmatrix}\\ &\quad\times\begin{pmatrix}1 & -1 & -1 & 1\\ 1 & 1 & -1 & -1\\ 1 & -1 & 1 & -1\\ 1 & 1 & 1 & 1\end{pmatrix}\\ &= \begin{pmatrix}-i & 0 & 0 & 0\\ 0 & 1 & 0 & 0\\ 0 & 0 & 1 & 0\\ 0 & 0 & 0 & i\end{pmatrix}. \end{aligned} \tag{6}$$

Thus, the operator of the whole pulse sequence is the conditional sign-flip operator with an overall phase factor of $e^{(-i\pi/4)}$ [17]

$$\begin{aligned}&\left(\frac{\pi}{2}\right)_y\left(\frac{\pi}{2}\right)_{-x}\left(\frac{\pi}{2}\right)_{-y}\left(\frac{\tau}{2}\right)(\pi)_{-x}\left(\frac{\tau}{2}\right)\\ &= e^{(-i\pi/4)}\begin{pmatrix}1 & 0 & 0 & 0\\ 0 & 1 & 0 & 0\\ 0 & 0 & 1 & 0\\ 0 & 0 & 0 & -1\end{pmatrix}.\end{aligned} \tag{7}$$

The state of the system after the conditional sign-flip is

$$|\psi_3\rangle = C_{11}|\psi_2\rangle = \frac{1}{2}\begin{pmatrix}1\\ 1\\ 1\\ -1\end{pmatrix}. \tag{8}$$

The density matrix of the system at this state, tomographed by the experiments of Fig. 1, is shown in Fig. 3. The experimental spectra are shown in Fig. 3g,h. The tomograph of the complete density matrix is given in Fig. 3i.

Inversion about mean can be implemented by a Hadamard operator H, a conditional phase shift C_{00} and another H [5].

$$\begin{aligned}D &= HC_{00}H = H\begin{pmatrix}-1 & 0 & 0 & 0\\ 0 & -1 & 0 & 0\\ 0 & 0 & -1 & 0\\ 0 & 0 & 0 & 1\end{pmatrix}H,\\ D &= \frac{1}{2}\begin{pmatrix}-1 & 1 & 1 & 1\\ 1 & -1 & 1 & 1\\ 1 & 1 & -1 & 1\\ 1 & 1 & 1 & -1\end{pmatrix}.\end{aligned} \tag{9}$$

It can be shown with similar analysis as above that the conditional phase shift C_{00} can be realized by the pulse sequence $(\frac{\pi}{2})_y(\frac{\pi}{2})_x(\frac{\pi}{2})_{-y}(\frac{\tau}{2})(\pi)_{-x}(\frac{\tau}{2})$ [10]. Hence the operator for 'D' is

$$\begin{aligned}D &= (\pi/2)_{-y}(\pi)_x\left(\frac{\pi}{2}\right)_y\left(\frac{\pi}{2}\right)_x\left(\frac{\pi}{2}\right)_{-y}\\ &\quad\times\left(\frac{\tau}{2}\right)(\pi)_{-x}\left(\frac{\tau}{2}\right)(\pi/2)_{-y}(\pi)_x.\end{aligned} \tag{10}$$

It may be mentioned that for implementing the above D (Eq. (9)), C_{00} gate is used due to the fact that the algorithm started with $|00\rangle$ pseudopure state. If one starts with $|ij\rangle$ pseudopure state, then the corresponding gate C_{ij} is required. After the step of *inversion about mean* we find the state of the system to be

$$|\psi_4\rangle = D|\psi_3\rangle = \frac{1}{2}\begin{pmatrix}0\\ 0\\ 0\\ 1\end{pmatrix}. \tag{11}$$

The measurement of the state will now give the searched state $|11\rangle$ with highest probability. This final state is again tomographed using the method of Fig. 1 and the result is shown in Fig. 3j,k. The diagonal elements give the amplitude of each state, whereas the off-diagonal elements represent the errors created by r.f. inhomogeneity and imperfection of pulses.

One can also combine the pulse sequences of *conditional sign-flip* and *inversion about mean* to a single pulse sequence, which can then be optimized to eliminate pulses that cancel. The simplified pulse sequence for a search of $|11\rangle$ is,

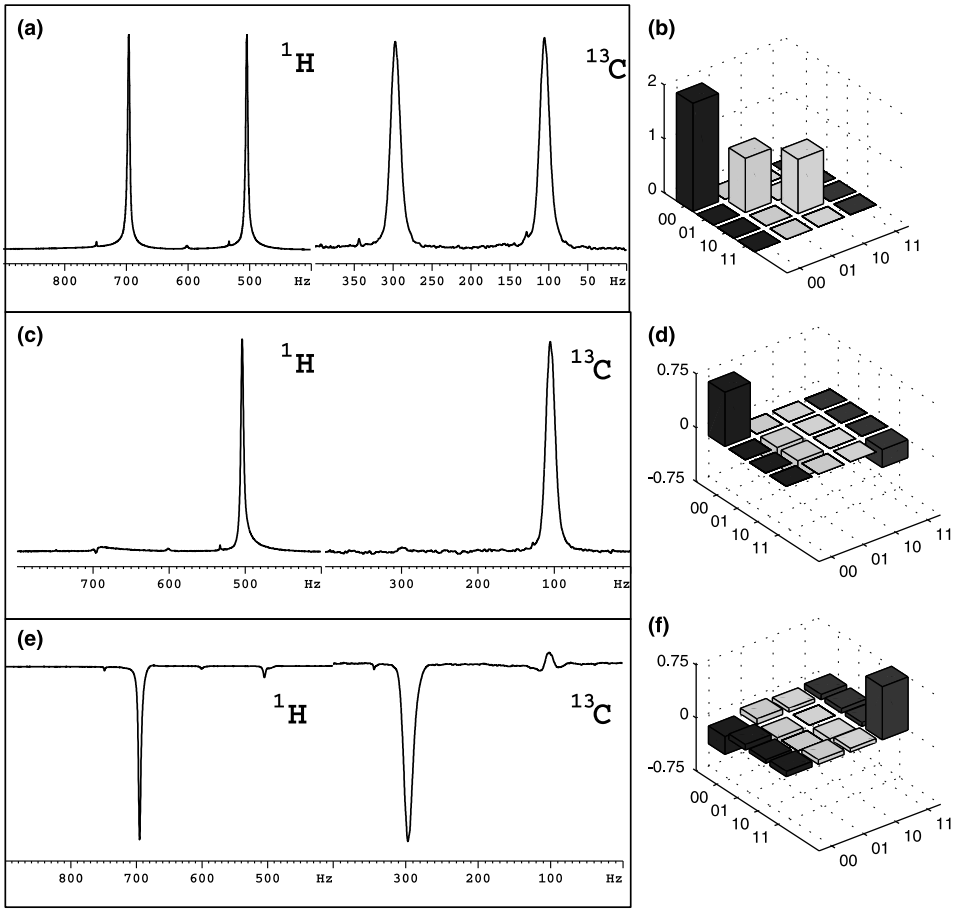

Fig. 4. Implementation of Grover's search algorithm using the optimized pulse sequence of Eq. (12). ^{1}H and ^{13}C spectra corresponding to (a) equilibrium, (c) pseudopure and (e) final searched states. (b), (d) and (f) are respective tomographs obtained using scheme of Fig. 1.

$$\left(\frac{\pi}{2}\right)_{-x}\left(\frac{\pi}{2}\right)_{-y}\left(\frac{\tau}{2}\right)(\pi)_x\left(\frac{\pi}{2}\right)_{-x}\left(\frac{\pi}{2}\right)_{x}\left(\frac{\pi}{2}\right)_{-y} \times \left(\frac{\tau}{2}\right)(\pi)_x\left(\frac{\tau}{2}\right). \quad (12)$$

The simplified pulse sequence for the search of all the possible four states ($|00\rangle, |01\rangle, |10\rangle$ and $|11\rangle$) have been shown by Chuang et al. [17]. We have performed the search of $|11\rangle$ state with the simplified pulse sequence. The equilibrium ^{1}H,^{13}C spectrum is shown in Fig. 4a and the tomograph of the equilibrium density matrix in Fig. 4b. The $|00\rangle$ pseudopure state is created by the method described earlier; the ^{1}H,^{13}C spectrum of the state is shown in Fig. 4c and its tomograph in Fig. 4d. After creation of uniform superposition on the above pseudopure state, the simplified pulse scheme of Eq. (12) is applied, yielding final searched state. The spectrum corresponding to the final searched state is given in Fig. 4e and its tomograph in Fig. 4f. The maximum error in the diagonal elements is 7% while that in the off-diagonal elements is 10%. This error is smaller than that obtained using separately the sequences for conditional sign flip Eq. (7) and inversion about average Eq. (10).

4. Conclusion

The experimental results demonstrate the use of 'efficient quantum state tomography using two-dimensional Fourier transform' to tomograph the system at initial, intermediate and final stages in

the implementation of Grover's search algorithm. While the previous method of tomography required 9 sets of experiments for a two-qubit system, we required only 2 sets. However, it is to be mentioned that one of the experiments is a two-dimensional experiment which requires a series of one dimensional experiments. But the novelty of the method lies in the fact that while the number of experiments in the earlier method rises exponentially with the number of qubits, this method requires the same number of experiments for any number of qubits or at best, to maintain the same level of digital resolution, the number of t_1 increments in the two dimensional experiment increases linearly with the number of qubits. It is understood that the new method will be of advantage for systems beyond four qubits. It may be noted that Grover's search algorithm has been reported earlier with 18% error [17]. The proposed method of tomography is less prone to errors since it uses hard pulses rather than spin selective pulses. While quantum information processing in larger systems is a daunting challenge, the novel method of 'efficient quantum state tomography' demonstrated here, provides an useful tool.

Acknowledgements

Useful discussions with Prof. K.V. Ramanathan and Mr. Neeraj Sinha are gratefully acknowledged. The use of DRX-500 NMR spectrometer funded by Department of Science and Technology, New Delhi, at the Sophisticated Instruments Facility, Indian Institute of Science, Bangalore, is also gratefully acknowledged.

References

[1] R.P. Feynman, Int. J. Theor. Phys. 21 (1982) 467.
[2] S. Lloyd, Science 273 (1996) 1073.
[3] D. Deutsch, R. Jozsa, Proc. R. Soc. London A 439 (1992) 553.
[4] P.W. Shor, in: Proceedings of the 35th Annual Symposium in Foundations of Computer Science, Santa Fe, NM, 1994, IEEE Computer Society Press, Los Alamitos, CA, 1994.
[5] L.K. Grover, Phys. Rev. Lett. 79 (1997) 325.
[6] D.G. Cory, A.F. Fahmy, T.F. Havel, Proc. Natl. Acad. Sci. USA 94 (1997) 1634.
[7] N.A. Gershenfeld, I.L. Chuang, Science 275 (1997) 350.
[8] Z.L. Madi, R. Bruschweiler, R.R. Ernst, J. Chem. Phys. 109 (1998) 10603.
[9] J.A. Jones, Prog. Nucl. Mag. Res. Spectrosc. 38 (2001) 325.
[10] N.A. Gershenfeld, I.L. Chuang, Quantum Computation and Quantum Information, Cambridge University Press, Cambridge, UK, 2000.
[11] T.S. Mahesh, A. Kumar, Phys. Rev. A 64 (2001) 012307.
[12] N. Sinha, T.S. Mahesh, K.V. Ramanathan, A. Kumar, J. Chem. Phys. 114 (2001) 4415.
[13] Y.S. Weinstein, M.A. Pravia, E.M. Fortunato, S. Llyod, D.G. Cory, Phys. Rev. Lett. 86 (2001) 1889.
[14] T.S. Mahesh, N. Sinha, K.V. Ramanathan, A. Kumar, Phys. Rev. A 66 (2002) 022313.
[15] T.S. Mahesh, K. Dorai, Arvind, A. Kumar, J. Mag. Reson. 148 (2001) 95.
[16] I.L. Chuang, N. Greshenfeld, M. Kubinec, D. Leung, Proc. R. Soc. Lond. A 454 (1998) 447.
[17] I.L. Chuang, N. Gershenfeld, M. Kubinec, Phys. Rev. Lett. 80 (1998) 3048.
[18] L.M.K. Vanderspypen, M. Steffen, M.H. Sherwood, C.S. Yannoni, R. Cleve, I.L. Chuang, Appl. Phys. Lett. 76 (2000) 646.
[19] Ranabir Das, T.S. Mahesh, Anil Kumar, Phys. Rev. A. (to be communicated).
[20] T.S. Mahesh et al., (manuscript under preparation).
[21] R.R. Ernst, G. Bodenhausen, A. Wokaun, Principles of Nuclear Magnetic Resonance in One- and Two-Dimensions, Clarendon Press, Oxford, UK, 1987.